Science of the Total Environment 921 (2024) 171027

Contents lists available at ScienceDirect

Science of the Total Environment

journal homepage: www.elsevier.com/locate/scitotenv

How data on transformation products can support the redesign of sulfonamides towards better biodegradability in the environment

Neele Puhlmann [a], Oliver Olsson [a,*], Klaus Kümmerer [a,b,*]

[a] Institute of Sustainable Chemistry, Leuphana University of Lüneburg, Universitätsallee 1, 21335 Lüneburg, Germany
[b] Research and Education Hub, International Sustainable Chemistry Collaborative Centre ISC_3, Germany

HIGHLIGHTS

- Transformation products (TPs) of sulfonamides (SUAs) inhibited bacterial luminescence.
- SUA-isomers & hydroxylated SUAs were eliminated in biodegradation test of TP-mixtures.
- Tested hydroxylated derivatives of sulfanilamide are not readily biodegradable (OECD 301F).
- No photo-TP was promising as a candidate for a better biodegradable SUA.

GRAPHICAL ABSTRACT

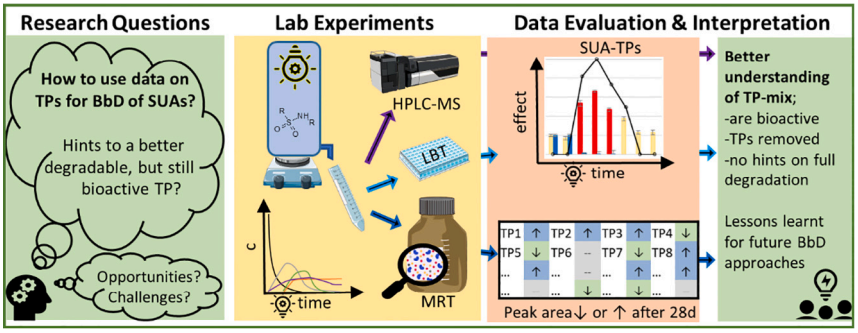

ARTICLE INFO

Editor: Jose Julio Ortega-Calvo

Keywords:
Benign
Design
Green
Persistence
Antibiotic
Active

ABSTRACT

Sulfonamide antibiotics (SUAs) released into the environment can affect environmental und human health, e.g., by accelerating the development and selection of antimicrobial resistant bacteria. *Benign by Design* (BbD) of SUAs is an effective risk prevention approach. BbD principles aim for fast and complete mineralization or at least deactivation of the SUA after release into the aquatic environment. Main objective was to test if mixtures of transformation products (TPs) generated via photolysis of SUAs can be used as an efficient way to screen for similarly effective but better biodegradable SUA alternatives.

Six SUAs were photolyzed (Hg ultraviolet (UV) light), and generated UV-mixtures analysed by high performance liquid chromatography coupled to an UV and tandem mass spectrometry detector. UV-mixtures were screened for antibiotic activity (luminescence bacteria test, LBT, on luminescence and growth inhibition of *Aliivibrio Fischeri*) and environmental biodegradability (manometric respirometry test, MRT, OECD 301F) using untreated parent SUAs in comparison. Additionally, ready environmental biodegradability of three commercially available hydroxylated sulfanilamide derivatives was investigated.

SUA-TPs contributed to acute and chronic bacterial luminescence inhibition by UV-mixtures. LBT's third endpoint, growth inhibition, was not significant for UV-mixtures. However, it cannot be excluded for tested TPs as concentrations were lower than parents' concentrations and inhibition by most parental concentrations tested was also not significant. HPLC analysis of MRT samples revealed that one third of SUA-TPs was reduced during incubation. Three of these TPs, likely OH-SIX, OH-SMX and OH-STZ, were of interest for BbD because the sulfonamide moiety is still present. However, hydroxylated sulfanilamide derivatives, tested to investigate the effect

* Corresponding authors.
E-mail addresses: oliver.olsson@leuphana.de (O. Olsson), klaus.kuemmerer@leuphana.de (K. Kümmerer).

https://doi.org/10.1016/j.scitotenv.2024.171027
Received 24 November 2023; Received in revised form 23 January 2024; Accepted 14 February 2024
Available online 19 February 2024

of hydroxylation on biodegradability, were not readily biodegraded. Thus, improving mineralization through hydroxylation as a general rule couldn't be confirmed, and no BbD candidate could be identified. This study fills data gaps on bioactivity and environmental biodegradability of SUAs' TP-mixtures. Findings may support new redesign approaches.

1. Introduction

Residues of sulfonamide antibiotics (SUAs) including their metabolites and transformation products (TPs) occur in the environment as a result of excretion by patients and treated animals and insufficient removal in wastewater treatment plants (WWTPs) (Baran et al., 2011; Felis et al., 2020; García-Galán et al., 2016; Spielmeyer, 2018). A recent study on pharmaceutical pollution in the world's rivers showed that the sulfonamide sulfamethoxazole (SMX) belongs to the contaminants with the highest concentrations out of 61 targeted active pharmaceutical ingredients. At 140 monitoring sites, the SMX concentration was above the predicted no-effect concentration, which may be of concern (Wilkinson et al., 2022).

Residues of SUAs can affect the environment and human health. Examples are the influence on the composition of microbial communities (Cycoń et al., 2019), phytotoxicity (Christou et al., 2018), and the development and selection of antimicrobial resistance especially in WWTP (Baran et al., 2011; Ezzariai et al., 2018; Felis et al., 2020). The latter is a serious global threat to human health. According to a risk-based assessment approach for WWTP effluents, SMX belongs to the top risk group using hazard units (Finckh et al., 2022). In order to reduce the development of resistance in patients, SUAs are often administered in combination with trimethoprim (e.g. as cotrimoxazole). Due to their inhibition of bacterial folic acid synthesis at two different sites, the antibacterial effect is improved.

Benign by Redesign of SUAs aims to develop a fast mineralizing SUA-derivative to avoid occurrence of SUA residues in the environment and associated effects. Like the *De-Novo Design* approach, *Benign by Redesign* belongs to the *Benign by Design* (BbD) concept (Kümmerer, 2007, 2010; Lorenz et al., 2021), which is based on the 10th principle of Green Chemistry, *Design for Degradation* (Anastas and Warner, 1998). BbD and other measures to tackle environmental pollution are proposed in the EU's Chemicals Strategy for Sustainability (European Commission, 2020a) and Pharmaceutical Strategy for Europe (European Commission, 2020b).

Lorenz et al. (2021) proposed a workflow to support the application of BbD, which begins with literature search on potential benign candidates. Useful literature data for the redesign of SUAs may be data on SUA-TPs that still contain the pharmacophore, i.e., the sulfanilamide structure. Reason is that slight structural transformation of the aniline ring could improve biodegradability, while preserving the bacteriostatic effect of SUAs due to sufficient structural similarity (Puhlmann et al., 2021). More than 600 SUA-TPs generated in laboratory experiments, WWTPs or the natural environment have been reported in literature (Puhlmann et al., 2022). However, no compound was identified to be of interest for BbD, mainly because of missing data for antibiotic activity and biodegradability.

Some hints taken from literature serve as good starting point for SUA's redesign. For example, *p*-OH-SMX, *p*-nitroso-SMX, *N4*-OH-SMX, and *p*-nitro-SMX were found to be bacteriostatic against *Aliivibrio fischeri* (Majewsky et al., 2014). This finding questions the necessity of the *p*-amino group of the pharmacophore for the bacteriostatic effect and expands the possibilities for BbD. During incubation of a photo-TP-mixture with sediment, *p*-nitro-SMX, the SMX-isomer, and a SMX-TP with opened isoxazole ring showed evidence of primary environmental biodegradation (Su et al., 2016). However, more data on mineralization rates is still needed to exclude the formation of environmentally persistent, possibly bioactive TPs, or even back-transformation to SMX. There are hints that *p*-nitro-SMX transforms back to SMX, like acetyl-SMX and glucuronide-SMX (Achermann et al., 2018; Radke et al., 2009; Su et al., 2016).

More data on a large pool of SUA-derivatives is needed to screen for a better biodegradable SUA. An effect-driven approach, starting with the synthesis of a pool of molecules within one step, provides a remedy for costly synthesis of SUA-derivatives, which are hardly commercially available, and their individual laborious testing. Such an approach consists of an *in vitro* testing of mixtures, generated e.g., by UV-irradiation, and focusing on those showing the desired effect (see e.g., Hensen et al., 2020; Rastogi et al., 2014). Suitable tests to screen UV-mixtures for antibiotic activity and environmental biodegradability are the 24 h luminescence bacteria test (LBT) according to Menz et al. (2013) and ready biodegradability tests according to the OECD series 301 (OECD, 2006). The 24 h LBT is typically used as ecotoxicity test, but also suitable to screen for antibiotic activity of SUAs' UV-mixtures. The reason is that Menz' 24 h LBT analyses not only acute ecotoxicity (luminescence inhibition, LI_{30min}) but also chronic ecotoxicity (LI_{24h}) and growth inhibition (GI_{14h}) of the gram-negative bacterium *Aliivibrio fischeri* (Menz et al., 2013). SUAs are administered also against gram-negative bacteria. Antibiotic activity tests may seem more suitable (e.g. Balouiri et al., 2016; Wiegand et al., 2008). However, they are using pathogenic bacteria, and this can be avoided for a first step of an effect-driven approach.

Given the state of research and methodology, primary aim of this study was to search for a TP that might be antibiotically active like the parent compound (PC) but better environmentally biodegradable than the PC. Secondary aim was to fill data gaps on the behaviour of SUAs and their TPs in biodegradability and ecotoxicity tests. Overall aim was to create a better understanding of possible opportunities and challenges of BbD. For this purpose, six SUAs (Fig. 1) were photolyzed as a means of non-targeted synthesis (cf. Lorenz et al., 2021) and generated UV-mixtures analysed by high performance liquid chromatography coupled to an UV and tandem mass spectrometry detector (HPLC-UV-MS^n). UV-mixtures were screened for bioactivity against *Aliivibrio*

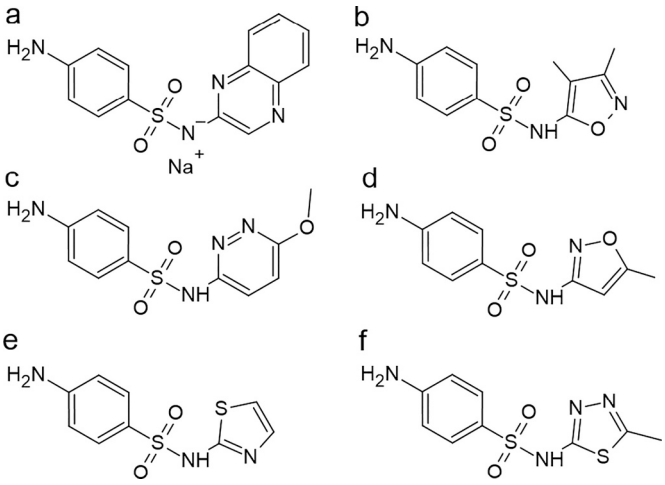

Fig. 1. Selection of parent compounds for the redesign of sulfonamides. a) sulfaquinoxaline-Na (SQX), b) sulfisoxazole (SIX), c) sulfamethoxypyridazine (SMP), d) sulfamethoxazole (SMX), e) sulfathiazole (STZ), f) sulfamethizole (SMT). The specific functional groups are: a) quinoxaline, b) 3,4-dimethyl-isoxazole, c) 6-methoxy-pyridazine, d) 5-methylisoxazole, e) thiazole, and f) 5-methyl-1,3,4-thiadiazole.

fischeri (luminescence bacteria test, LBT) and environmental ready biodegradability (manometric respirometry test, MRT, OECD 301F). In addition, sulfanilamide (SAA) and commercially available hydroxylated SAA-derivatives (Fig. 2) were tested for ready biodegradability to examine the rule of thumb that hydroxylation favours biodegradability (Boethling et al., 2007).

2. Method

2.1. Test compounds and other chemicals

Six SUAs (Fig. 1, $c_0 = 50$ mg L^{-1}) were photolyzed to create diverse TP-mixtures with fast decrease in concentration of the PC: sulfaquinoxaline-Na (SQX), sulfisoxazole (SIX), sulfamethoxypyridazine (SMP), sulfamethoxazole (SMX), sulfathiazole (STZ), sulfamethizole (SMT). Selection of SUAs covered various specific functional groups at the pharmacophore, i.e., the SAA structure, with regard to the size of the aromatic rings, heteroatoms and substituents at the rings (Fig. 1).

Three hydroxylated SAA-derivatives (Fig. 2) were selected for additional biodegradability testing (MRT). All chemicals used in this study are listed in the supporting information (SI; Table S1).

2.2. Stock solution and dilution series

To prepare a SUA stock solution of 50 mg L^{-1}, 50 mg SUA were solved in about 800 mL ultrapure water. Then, pH was increased up to pH 10 using NaOH solution (0.1 M) to facilitate the dissolution of SUAs in water. Once the solution was homogenous, pH was set to pH 7 with HCl solution (0.1 M) before filling up to 1 L. SUAs remained in solution. The stock solution was diluted with water in 8 steps for later use in the LBT: 50, 40, 30, 20, 10, 5, 2.5 and 1.25 mg L^{-1}. The dilution was stored at −20°C until the use in the LBT (see Section 2.5).

2.3. Generation of SUA-TPs by photolysis

SUAs were photo-transformed according to the method described by Rastogi et al. (2014). 800 mL stock solution (see Section 2.2) were irradiated for 256 min with a medium pressure mercury UV light source (TQ 150; UV lamp, Consulting Peschl, Mainz, Germany; λ = 200–600 nm) at 20 ± 1°C and pH 7 ± 1. To ensure a stable temperature during the experiment, the lamp was housed in a water-cooled quartz glass tube (cooling system WKL230, LAUDA, Berlin, Germany). pH was kept constant using NaOH solution (0.1 M). While stirring continuously, samples were drawn from the reactor in an exponential series (0, 2, 4, 8, 16, 32, 64, 128, 256 min; samples SUA-X, with X = irradiation time) and used for HPLC-UV-MS^n analysis and the LBT. Samples were stored at −20°C until the HPLC-UV-MS^n analysis and LBT.

2.4. HPLC-UV-MS^n analysis

Removal rates of the PC and related concentration-time courses (c-t courses) of the formed photo-TPs were monitored. Typical for TPs are c-t courses that show first a formation phase and then further transformation/degradation or constant concentration while the parent compound is primarily degraded. Thus, a peak is considered a SUA-TP in case of monitored peak areas that are increasing and then decreasing or are constant along the irradiation time. The used analytical system was an Agilent 1100 series HPLC system (Agilent Technologies, Waldbronn, Germany) coupled to an UV–Vis detector and a Bruker Daltonic Esquire 6000 + ion-trap Mass Spectrometer with electrospray ionization interface (Bruker Daltonics, Bremen, Germany). Reversed phase (Accucore C18–2.6, 100/2.1, Thermo Scientific) gradient method was applied using 0.1% formic acid and acetonitrile (gradient see SI, Section 2). Column oven temperature was set to 40°C, the injection volume to 10 μL of 1:10 diluted samples, and flow rate to 0.25 mL min^{-1}. MS^n was operated in full-scan mode.

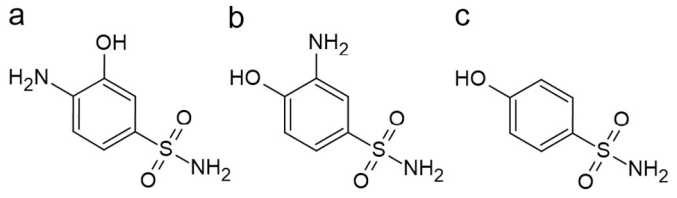

Fig. 2. Commercially available sulfanilamide-derivatives. a) 4-amino-3-hydroxybenzenesulfonamide (4A3OH-BS), b) 2-aminophenol-4-sulfonamide (2AP4-S), c) 4-hydroxybenzenesulfonamide (4OH-BS).

TPs were named according to their retention time and *m/z* in brackets. No brackets indicate that the TP was detected solely by UV. Due to the lack of TP-standards, quantification was not possible. Amount was expressed as relative peak area (rel. PA; $PA_{TP}/PA_{PCinSUA-0}$ or $PA_{TP}/PA_{TP,max}$).

Structures were proposed provisionally based on MS^1 and MS^2 data, including differences in m/z to PC and isotope peaks (particularly ^{34}S indicating presence of SUA moiety) and fragment ions. Supportively, literature data on TPs and transformation processes of PC was used (e.g., Bonvin et al., 2013; Boreen et al., 2004, 2005; Zhou and Moore, 1994). We need to stress that only BbD candidates would have been prioritized for structure elucidation for this BbD approach (see intro on effect-driven approach).

2.5. Luminescence bacteria test (LBT)

Based on EN ISO 11348, Menz et al. (2013) developed a special luminescence bacterium test (LBT) to assess not only acute but also chronic inhibition of bacterial luminescence (LI_{30min}, LI_{24h}). The growth inhibition after 14 h (GI_{14h}) can be evaluated by this method, which indicates bacteriostatic effects. Moreover, no pathogenic bacteria are used in contrast to typical activity tests for antibiotics (e.g., Balouiri et al., 2016; Wiegand et al., 2008). For these reasons and also because the test is quick and simple while having a high level of standardization, SUAs and UV-mixtures were investigated using Menz' 24 h test. Note, SUAs' half maximal effective concentration (EC_{50}) for GI_{14h} are known to be higher than SUA's concentration set in this study design. Nevertheless, we decided to use lower concentrations because preceding photolysis was more efficient at lower concentrations, water solubility was assured and fewer resources were consumed. Moreover, this endpoint served as a first screening to identify those TPs that are bacteriostatic at lower concentrations than the PC, i.e., more active. For example, EC_{50} of SMX and *p*-nitro-SMX for GI_{14h} in Menz' 24 h LBT performed by Majewsky et al. (2014) were 599 μmol L^{-1} (= 152 mg L^{-1}) and 28 μmol L^{-1} (= 5.8 mg L^{-1}), respectively. From pharmaceutical perspective, high activity enabling a lower dose which may reduce the risks for side effects can be advantageous.

To investigate if TPs of the UV-mixtures inhibit luminescence or growth of *Aliivibrio fischeri*, measured inhibition of UV-mixtures ($I_{measured}$) was compared to the theoretical inhibition attributed to the PC residue in the sample ($I_{theoretical}$). The theoretical inhibition was derived from dose-response relationship of measured dilution series of the SUA stock solution (see Section 2.2, with $n = 3$ replicates). TPs occurring in the UV-mixture were suspected to contribute to bacterial luminescence or growth inhibition if measured inhibition by this mixture was significant (≥20% according to Menz et al., 2013) and ≥ 6% higher than the theoretical inhibition by the PC residue (threshold of 6% set based on authors' experience):

$$\Delta\text{Inhibition } \Delta I = I_{measured} - I_{theoretical} \geq 6\%.$$

To investigate if the effects can be attributed to specific TPs the evolution of the inhibitory effect associated with TPs (when $\Delta I \geq 6\%$.) was compared to concentration-time courses of TPs determined by

HPLC-UV-MS^n.

For each SUA, the dilution series of the SUA stock solution (7–8 steps, see Section 2.2) and the UV-mixtures (8–9 irradiation time points, see Section 2.2) were tested in one test run. Eight (0–128 min) instead of nine UV-mixtures (0–256 min) were tested for those SUAs where no transformation was observed anymore from 128 to 256 min, i.e., SUA-256 equalled SUA-128. Before performing the LBT, samples were salted up to 2% NaCl to create right conditions for this marine bacterium. Their pH and peroxide content were controlled to be at pH 7 ± 1 and < 0.5 mL^{-1} (H_2O_2 equivalents), respectively.

The overnight culture of *Aliivibrio fischeri* NRRL-B-11177 (Hach-Lange GmbH, Düsseldorf) was prepared in culture medium (details in SI, Section 2.1) and incubated at 21°C and 150 rpm for 21 ± 0.5 h. The overnight culture was diluted with fresh culture medium to an initial density of 20 formazine turbidity units (FTU). Aliquots of 100 μL of this main culture were transferred into a 96-well microplate (100 mL of culture medium for negative controls, NC). Initial luminescence emission and optical density (578 nm) were measured after 30 min pre-incubation at 15°C. Subsequently, the test culture (or culture medium for NC) was supplemented with 100 μL of the respective sample (SUA test samples (n = 3), 2% NaCl for blanks (n = 16) and NC (n = 8), 2 positive controls (2*n = 2*4)). This resulted in a dilution factor of 2 for all test samples and 25 mg L^{-1} as the highest SUA concentration).

Continuously, luminescence and optical density were measured for 24 h at 15°C (Menz et al., 2013).

2.6. Manometric respirometry test (MRT)

The manometric respirometry test (MRT, OECD 301F) was performed using activated sludge taken from the municipal WWTP in Lüneburg, Germany in December 2022 and January 2023 to investigate biotic removal of SUA-TPs (OECD, 2006). TPs were tested as a UV-mixture of one specific UV-irradiation timepoint (see photolysis). The irradiation timepoint was selected based on a high number of photo-TPs and low PC residue to test as many TPs as possible at higher concentrations and less impacted by the PC. Biodegradability of the unirradiated solution (SUA − 0) was tested as well to serve as reference for later evaluation. Parallel determination was performed for all samples (n = 2). For this purpose, all reagents for the test preparation were combined in one bottle and only divided into two bottles at the start of incubation.

Sample concentration was adjusted to give a theoretical oxygen demand (ThOD) of approx. 30 mg L^{-1}. ThOD factors ($m_{oxygen}/m_{compound}$; for SUAs see SI, Section 2.2) of UV-mixtures cannot be calculated as the molecular formulas and composition in the mixture are unknown. Approximately, the same ThOD as the one of PC was taken. Preceding results of a photometric cell test on the chemical oxygen demand of five UV-mixtures (SIX-16, SMP-64, SMX-8, STZ-16, SMT-16) showed that this simpler and less resource intensive method is a good approximation (SI, Table S2).

Non-purgeable organic carbon (NPOC) and oxygen concentrations were measured, the latter continuously, to calculate mineralization rates based on NPOC removal and oxygen demand, respectively. NPOC was measured at d0 and d28 using a TOC-analyzer (TOC-V CPH/CPN, Shimadzu, Duisburg, Germany). The thresholds for ready biodegradability are 60% of ThOD or 70% removal of dissolved organic carbon (considered NPOC). Thresholds must be reached in a 10-days window within the incubation of 28 days (OECD test series 301). HPLC-UV-MS^n analysis (described above) of MRT samples from d0 and d28 of incubation was performed to identify TPs with constant, increased or reduced PA after incubation. Sterile control (no inoculum added) supported differentiation of biotic processes and sorption on sludge to abiotic transformation.

Analogously, SAA and hydroxylated SAA-derivatives (Fig. 2) progressed through the MRT. ThOD factors can be found in SI (Table S2).

2.7. Identifying TPs of interest for BbD

Structures of interest for BbD should be similar to the parent on the one hand, e.g., still contain the pharmacophore. On the other hand, a structure of interest should be modified sufficiently to result in better biodegradability. For example, modification of the SAA structure may improve biodegradability in contrast to slight modification of the specific functional group, e.g., resulting in isomers. The rational is that the entire group of SUAs with diverse specific functional groups at the sulfonamide group is not readily biodegradable in the environment (National Center for Biotechnology Information, 2023a, 2023b, 2023c; and own data not published), and a TP structure that is slightly modified only at the specific functional group is expected to belong to this group of not readily biodegradable compounds. Therefore, these structural features, indicated by MS^1 data, excluded a TP as candidate for BbD:

- lost pharmacophore, i.e., SAA, indicated by missing ^{34}S isotope peak for the sulfonamide moiety and m/z < 173 (m/z of SAA).
- same m/z as SUAs, i.e., SUA-isomers as they are likely to be similarly resistant to biodegradation as the PC.

Remaining structural-suitable TPs were of interest for BbD if they were identified in the LBT as possibly contributing to the inhibitory effect of their UV-mixture or detected with decreased PA after 28 days of MRT. TPs of interest were investigated and discussed in more detail to gain further insights. A BbD candidate would meet both criteria.

TPs detected only by the UV detector, i.e., not by MS, lacked structural information. They were prioritized for closer examination, only if both criteria, i.e., contributing to the inhibitory effect (LBT) and decreasing in PA (MRT), were met.

Independent of BbD interest, all TPs were considered to interpret MRT and LBT results of the whole UV-mixture.

3. Results and discussion

3.1. Generation of photo-TPs of sulfonamides

HPLC analysis of UV-mixtures showed that primary elimination of the parent compound was completed by 64 min UV-irradiation for all except SMP (256 min) and SQX (almost by 256 min) (SI, Fig. S1). In total 66 photo-TPs, 8–15 TPs per SUA, were detected in the UV-mixtures, some of them only by UV-detection, i.e. not by MS^n (Table 1). MRT samples of one specific irradiation timepoint (SQX: 64 min, SIX: 16 min, SMP: 64 min, SMX: 8 min, STZ: 16 min, SMT: 16 min) contained most of them (Table 1, first column). Concentration-time courses of TPs can be found in SI (Figs. S2–S7).

The mass spectrum of 19 TPs did not show the ^{34}S isotope peak of the sulfonamide moiety clearly indicating the loss of the pharmacophore for these TPs (Table 1).

Several detected TPs were in line with well-known transformation processes occurring during UV-irradiation of SUAs such as δ-cleavage, hydroxylation, desulfonation, oxidation, e.g., of the *p*-amino group, and isomerization (e.g., Boreen et al., 2004, 2005; Zhou and Moore, 1994). Among them were:

- amines of the specific functional group (NH_2-R; 2-amino-quinoxaline of SQX, 5-amino-3,4-dimethylisoxazole of SIX, 3-amino-6-methoxy-pyridazine of SMP, 3-amino-5-methyl-isoxazole of SMX, 2-amino-thiazole of STZ, 2-amino-5-methyl-1,3,4-thiadiazole of SMT),
- hydroxylated SUAs (OH-SQX, -SIX, -SMP, -SMX, -STZ, -SMT),
- desulfonated SUAs (desulfo-SQX, -SMP, -SMX, -SMT),
- nitroso-SUAs (NO-SQX, NO-SMP), and
- SUA-isomers (3 SIX-isomers, SMP-isomer, SMX-isomer, STZ-isomer).

To the best of our knowledge, detected SIX-isomers (m/z = 268; see SI, Figs. S8a,b and S9a,b) and the SMP-isomer (m/z = 281) are not yet

Table 1
SUA-TPs detected in UV-mixtures. Row on occurrence: timepoint of concentration peak in brackets. MRT: TP detected in UV-mixture used for MRT; na: not applicable for this TP as UV-detection only; $\Delta m/z$: m/z_{TP} - m/z_{PC}.

PC	TP named with retention time (and m/z detected by MS)	Occurrence during irradiation/min	^{34}S peak in MS^1 indicating intact SUA moiety	Literature describing the same m/z of the ion (MS^1)	Structure proposal based on MS^n (incl. fragments from MS^2) and literature
	TP-2.9 (146) MRT	8–256 (128)	no	Ji et al., 2017; Nassar et al., 2018; Qiu et al., 2019; Urbano et al., 2017b; Urbano et al., 2017a	2-amino-quinoxaline
	TP-7.3 (317) MRT	8–128 (16, 128)	yes	Liao et al., 2016; Qiu et al., 2019	OH-SQX
	TP-7.8 (237) MRT	2–256 (64)	no	Liao et al., 2016; Nassar et al., 2018	desulfo-SQX
	TP-10.3 (238) MRT	16–256 (16)	no		$\Delta m/z$: −63, desulfo-4-OH-SQX
SQX	TP-10.7 (315) MRT	16–256 (128)	yes		NO-SQX
	TP-3.2 MRT	8–256 (128)	na		na
	TP-4.7	64–128 (128)	na		na
	TP-9.5	4–128 (32)	na		na
	TP-14.1	16–128 (32)	na		na
	TP-15.2	16–128 (64)	na		na
	TP-16.0	32–256 (32)	na		na
	TP-16.2	16–256 (32)	na		na
	TP-1.2 (286) MRT	2–16 (4)	yes		Δm/z: +18 (1)
	TP-1.4 (173) MRT	8–256 (16)	yes	Many, e.g., Baena-Nogueras et al., 2017	SAA
	TP-1.5 (113)	64–256 (128)	no	Ge et al., 2019; Yang et al., 2010	5-amino-3,4-dimethylisoxazole
	TP-3.2 (286) MRT	2–32 (4)	yes		Δm/z: +18 (2)
	TP-6.2 (268) MRT		yes	cf. SMX-isomers by Palm et al., 2023	SIX-isomer (1)
	TP-7.0 (140) MRT	8–16 (8)	no	Wang et al., 2021	nitrophenol
	TP-7.0 (268) MRT	4 (4)	yes	cf. SMX-isomers by Palm et al., 2023	SIX-isomer (2)
SIX	TP-10.3 (284) MRT	32–256 (128)	yes	Baena-Nogueras et al., 2017; Ge et al., 2019; Yao et al., 2017	OH-SIX
	TP-10.9 (268) MRT	8–256 (16)	yes	cf. SMX-isomers by Palm et al., 2023	SIX-isomer (3)
	TP-12.3 (378)	2–4 (2)	yes		$\Delta m/z$: +110
	TP − 0.9 MRT	4–256 (8)	na		na
	TP-1.3	16–32 (16)	na		na
	TP-1.8 MRT	8–256 (32)	na		na
	TP-3.2 MRT	4–64 (4)	na		na
	TP-4.2	8–64 (16)	na		na
	TP-1.3 (126) MRT	4–256 (128)	no	Nassar et al., 2017	3-amino-6-methoxypyridazine
	TP-2.4 (233) MRT	16–256 (128)	no		OH-desulfo-SMP
	TP-3.2 (217) MRT	0–256 (64)	no	Gao et al., 2019	desulfo-SMP
	TP-3.9 (297) MRT	8–256 (32)	yes	Gao et al., 2019; Khaleel et al., 2013	OH-SMP (1)
SMP	TP-4.8 (245) MRT	128–256 (256)	no		$\Delta m/z$: −36
	TP-8.1 (297)	8–128 (32)	yes	Gao et al., 2019; Khaleel et al., 2013	OH-SMP (2)
	TP-9.1 (295) MRT	16–256 (64,128)	yes	Gao et al., 2019; Khaleel et al., 2013	NO-SMP
	TP-10.2 (281)	32–256 (128)	yes		SMP-isomer
	TP − 0.9 MRT	8–256 (64–256)	na		na
	TP-1.1 MRT	MRT only	na		na
	TP-1.0 (99) MRT	MRT only	No	Many; well elucidated by Zhou and Moore, 1994	3-amino-5-methyl-isoxazole
	TP-1.1 (190)	4–16 (8)	no	Baena-Nogueras et al., 2017; Bonvin et al., 2013; Liu et al., 2020	desulfo-SMX
	TP-1.3 (286) MRT	4–32 (8)	yes	Fabbri et al., 2019; Gómez-Ramos et al., 2011; Liu et al., 2020	OH-OH-SMX
	TP-1.5 (246)	4–8 (4)	no	Wang et al., 2020	Δm/z: −8
	TP-1.9 (216)	4–8 (8)	yes		Δm/z: −38
SMX	TP-1.9 (99) MRT	MRT only	no	Boreen et al., 2004; Zhang et al., 2016	2-amino-5-methyloxazole
	TP-4.1 (254) MRT	2–16 (4)	yes	Many; well elucidated by Zhou and Moore, 1994	SMX-isomer
	TP-9.5 (270) MRT	4–16 (8)	yes		OH-SMX
	TP − 0.9 MRT	4–256 (16)	na		na
	TP-1.1 MRT	4–256 (16)	na		na
	TP-2.1 MRT	4–16 (8)	na		na
	TP-2.4	4–8 (4,8)	na		na
	TP-10.3	4–8 (8)	na		na
	TP-1.1 (140)	4–32 (8)	yes		Δm/z: −116
	TP-1.1 (101) MRT	4–64 (16)	no	Baena-Nogueras et al., 2017; Boreen et al., 2004; Ge et al., 2019; Niu et al., 2017	2-aminothiazole
	TP-1.4 (94)	16–64 (32)	no	Deng et al., 2019; Hu et al., 2021	aniline
STZ	TP-3.6 (272) MRT	0–16 (8)	yes	Baena-Nogueras et al., 2017; Calza et al., 2004; Ge et al., 2019	OH-STZ
	TP-7.3 (256) MRT	4–32 (8)	yes	Spielmeyer et al., 2015	STZ-isomer
	TP-9.0 (170)	4–32 (4)	no		Δm/z: −86
	TP-1.1 MRT	0–256 (32)	na		na
	TP-1.3	8–16 (8)	na		na
SMT	TP-1.2 (116) MRT	2–256 (16)	no	Baena-Nogueras et al., 2017; Boreen et al., 2004; Klauson et al., 2010	2-amino-5-methyl-1,3,4-thiadiazole
	TP-1.7 (233)	16–256 (16)	yes		Δm/z: −38

(*continued on next page*)

Table 1 (*continued*)

PC	TP named with retention time (and m/z detected by MS)	Occurrence during irradiation/min	^{34}S peak in MS^1 indicating intact SUA moiety	Literature describing the same m/z of the ion (MS^1)	Structure proposal based on MS^n (incl. fragments from MS^2) and literature
	TP-2.0 (207) ^{MRT}	4–32 (8)	no	Baena-Nogueras et al., 2017	desulfo-SMT
	TP-3.5 (312) ^{MRT}	2–16 (4)	yes		Δm/z: +4
	TP-4.3 (158) ^{MRT}	8–64 (16,32)	no		4-aminobenzenesulfinate
	TP-7.7 (287) ^{MRT}	4–16 (8)	yes	Klauson et al., 2010	OH-SMT
	TP − 0.9 ^{MRT}	2–256 (16)	na		na
	TP-3.4	16–128 (64)	na		na

described in literature. Given structural similarity between SIX and SMX (both are isoxazoles) it is plausible that the isoxazole ring of SIX could isomerize to oxazole like SMX for which the photo-isomer 4-amino-*N*-(5-methyl-2-oxazolyl)benzenesulfonamide is well studied (Zhou and Moore, 1994). SMX and this photo-isomer can be present in amine or imine structure due to enamine-imine tautomerization, leading to four structures with the same molecular formula (Palm et al., 2023). Same tautomerization could also justify the detection of four structures with m/z of SIX = 268 (Fig. 3).

Many TPs (about 75%) that were detected by UV only are expected to be very polar because of short retention times on the reversed phase.

3.2. Luminescence bacteria test (LBT)

Menz' 24 h luminescence bacteria test (LBT) was suitable to determine differences between PCs and TPs in mixtures with respect to their acute and chronic luminescence inhibition (LI_{30min}, LI_{24h}).

Acute luminescence inhibition (LI_{30min}) was not significant for all tested SUAs even at the highest test concentrations of 25 mg L^{-1}. In contrast, UV-mixtures of SMP, SMT, and STZ showed significant LI_{30min} (≥ 20% inhibition) that can therefore be attributed to the TP portion of the UV-mixture (Fig. 4). The concentration-time courses of one SMP-TP and five STZ-TPs matched the evolution of LI_{30min}, indicating possible contribution of such TPs to the inhibitory effect. However, there was no match for a SMT-TP (Fig. 4, and Table 2, upper part).

Chronic luminescence inhibition (LI_{24h}) by PCs was in general much higher than LI_{30min}. Maximum LI_{24h} by all PCs was about 80% except SMT with 40% (dose-response curves in SI, Section 3.2). Significant LI_{24h} attributed to the TP portion was found for several UV-mixtures of all SUAs, namely SQX-32-256, SIX-16, SMP-64-256, SMX-32-128, SMT-8-128 and STZ-8-32. Several specific TPs that could have contributed to LI_{24h} due to their concentration-time courses were identified for all of these UV-mixtures, except those of SQX and SMT (Table 2, middle part, Fig. 5).

Growth inhibition (GI_{14h}) by PCs was very low (< 30% by highest c of 25 mg L^{-1}). GI_{14h} by SMT was not significant (< 20% by 25 mg L^{-1} SMT). Based on ΔGI_{14h}, no UV-mixture indicated highly active TPs that resulted in significant GI_{14h} (SI, Section 3.2). This doesn't signify that UV-mixtures didn't contain bacteriostatic TPs, considering very low GI_{14h} by PCs which were tested in higher concentration than their resulting TPs by default.

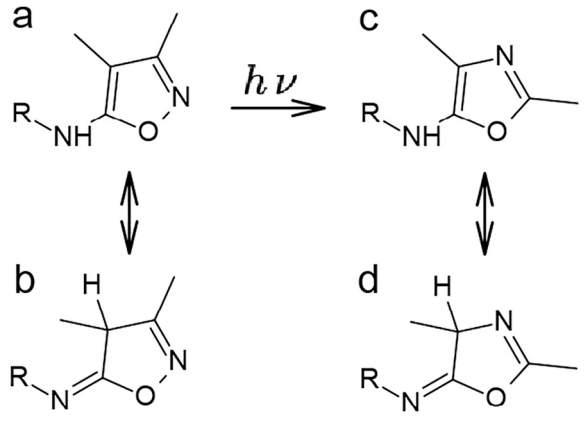

Fig. 3. SIX (a, b) and its photo-isomers (c, d) proposed as amine (a, c) or imine (b, d) structure (compare SMX-isomers by Palm et al., 2023), with R-NH_2 = Sulfanilamide.

3.2.1. Insights from LBT

UV-mixtures resulting from photolysis of SMP (256), STZ (4–16) and SMT (16, 128) showed significant acute luminescence inhibition (LI_{30min}) attributed to the TPs in the UV-mixture. 5 STZ-TPs and 1 SMP-TP were suspected being contributing to LI_{30min}. This includes the STZ-isomer TP-7.3 (256).

STZ-TP-7.3 (256) could be promizole, an antituberculotic, that was identified by Spielmeyer et al. (2015) as the main TP after UV-irradiation of STZ. Promizole was less microbially active than STZ in the Brilliant Black Reduction Maximum Residue Level test (EC_{50}: 250 μg/L vs 50 μg/L) (Spielmeyer et al., 2015). This is not in contrast to our findings as another mechanism of action for this bioactive compound could lead to LI_{30min}. Moreover, promizole lacks the sulfonamide structure because of a direct bond between the sulfonyl group and the thiazole ring, indicating another mechanism of action apart from the inhibition of the dihydropteroate synthase.

TP-4.8 (245) is the only SMP-TP identified as potentially bioactive. It is not reported in literature to the best of our knowledge. SMP-TP-4.8 (245) could also contribute to LI_{24h}. Missing ^{34}S isotope peak in the mass spectrum indicates the loss of the sulfonamide moiety and thus a mechanism of action apart from the inhibition of dihydropteroate synthase.

Chronic luminescence inhibition (LI_{24h}) by TPs in the UV-mixture was found for SQX-32-256, SIX-16, SMP-64-256, SMX-32-128, STZ-8-32 and SMT-8-128. In these UV-mixtures, 4 SIX-TPs, 1 SMP-TP (see previous paragraph), 2 SMX-TPs and 1 STZ-TP were identified tentatively being contributing to LI_{24h}. This includes the newly identified SIX-isomer TP-10.9 (268). Structural similarity to SIX (Figs. 1b, 3) hints at bioactivity due to same mechanism of action.

Among detected SMX-TPs, the only TPs that could contribute to LI_{24h} by mixtures SMX-32-128 were TP-0.9 and TP-1.1. Desulfo-SMX, the SMX-isomer and OH-SMX are considered bioactive according to literature, but were not detectable anymore in the bioactive UV-mixtures from 32 min onwards (Table 1, row "Occurrence during irradiation"). Desulfo-SMX was found to contribute potentially to the growth inhibition of *E. coli* by a TP-mixture generated by photocatalysis (catalyst Fe_3O_4-ZnO@g-C_3N_4, low energy-consuming UV lamp, pH = 7) (Mirzaei et al., 2018). The SMX-isomer was similarly bioactive compared to SMX in the Brilliant Black Reduction Maximum Residue Level test (Spielmeyer et al., 2015). *N4*-OH-SMX was found to be similarly bacteriostatic against *Aliivibrio fischeri* as SMX, showing an EC_{50} value of 200 mg L^{-1} (Majewsky et al., 2014). *p*-OH-SMX, *p*-nitroso-SMX, and *p*-nitro-SMX, that are bacteriostatic against *Aliivibrio fischeri* (Majewsky et al., 2014), were not detected in this study.

Comparing the c-t courses of STZ-TPs and ΔLI_{24h} development, indicated STZ-TP-1.1 (101) to contribute to ΔLI_{24h} in mixtures STZ-8-32 (max at 16 min) due to maximum PA at 16 min. However, this is a good example to stress that, albeit such identification based on c-t courses, the

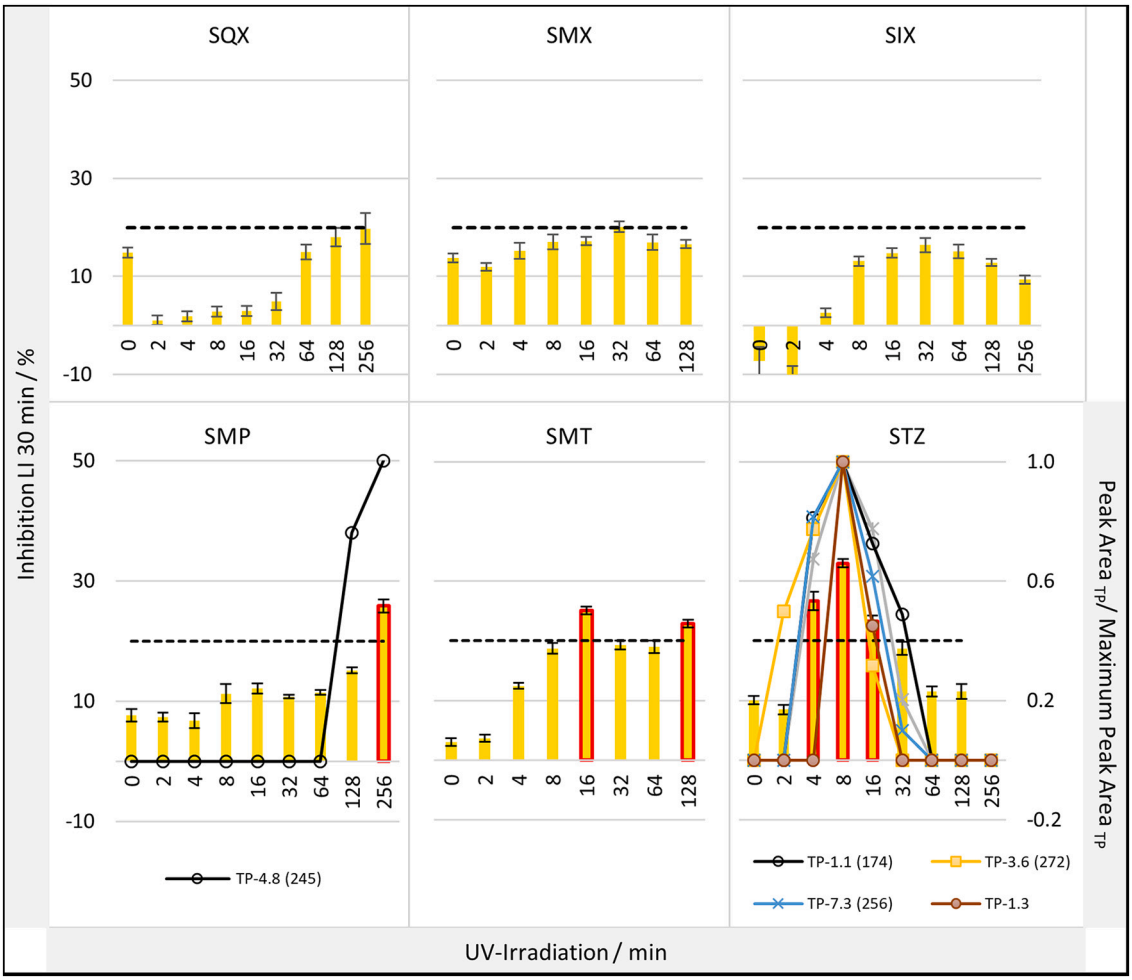

Fig. 4. Acute luminescence inhibition (LI_{30min}) by UV-mixtures of SUAs (yellow bars), and concentration-time courses of possibly bioactive TPs of SMP and STZ. Significant LI_{30min} by UV-mixtures of SMP, SMT, and STZ can be attributed to the TP portion of the UV-mixture (red bordered) because of non-significant initial LI_{30min} even by SUA-0 with highest concentration of 25 mg SUA L^{-1}. Threshold for significant inhibition is 20% (dashed line). Raw data can be found in SI (Section 3.2).

Table 2
TPs that could have contributed to luminescence inhibition (LI_{30min}, LI_{24h}). Reasoning was most often a c-t course of the TP with maximal concentration in the UV-mixture showing also maximal ΔLI (see*).

	Sample SUA-X, with X = irradiation / min	Possibly Contributing TPs		
		without SUA moiety	with SUA moiety, or an isomer	no data on structure
LI_{30min}	SMP-256	4.8 (245)*		
	SMT-16, −128	***		
	STZ-8	1.1 (140)*	1.1 (174)* 3.6 (272)* 7.3 (256)*	1.3*
	SQX-32-256	***		
	SIX-16		1.4 (173)* 10.9 (268)*	1.3* 4.2*
LI_{24h}	SMP-64-256	4.8 (245)*		
	SMX-32-128			0.9** 1.1**
	SMT-8-128	***		
	STZ-32-128	1.1 (101)*		
Reasoning	*max c in the UV-mixture of max ΔLI. **present in samples where ΔLIs were of constant magnitude. ***No TP was detected with a c-t course that could explain the evolution of ΔLI.			

entire UV-mixture needs to be reviewed, especially as additive, synergistic and other mixture effects can result in measured LI_{24h}. For example, TP-7.3 (256) may also have contributed to LI_{24h}, possibly even to higher extent than TP-1.1 (101), although its c-t course didn't match the development of ΔLI_{24h} (PA_{max} at 8 min and not 16 min). The reason for this consideration is that PA_{16min} of TP-7.3 (256) was still greater compared to other TPs ($PA_{16min}/PA_{STZ,0}$ = 3.9% versus < 1% for other TPs, see SI, Fig. S6), suggesting a high TP share. Moreover, TP-7.3 (256) is proposed to be promizole, the main photo-TP of STZ and a bioactive compound (see above).

In general, the identification of TPs that might contribute to the effect based on their c-t courses is challenging because of the variety of detected TPs. Non-detectable TPs could also contribute to the measured effect. Other effects than the inhibition of the dihydropteroate synthase can cause luminescence inhibition, especially by TPs that lost the sulfonamide moiety. In addition, effects can be additive, synergistic or antagonistic. Moreover, concentrations of TPs are unknown but expected to be rather low, especially when the PC is transformed into many different TPs to an equal extent. Therefore, indication of TPs that contributed to the bacterial inhibition need further proof to understand ecotoxicity of single TPs, but was supportive for the identification of TPs of interest for BbD (see Section 4).

Growth inhibition (GI_{14h}) by PCs was low or not significant as expected for tested concentration range because the concentration was not higher than 25 mg L^{-1} whereas, for example, the EC_{50} of SMX was 152

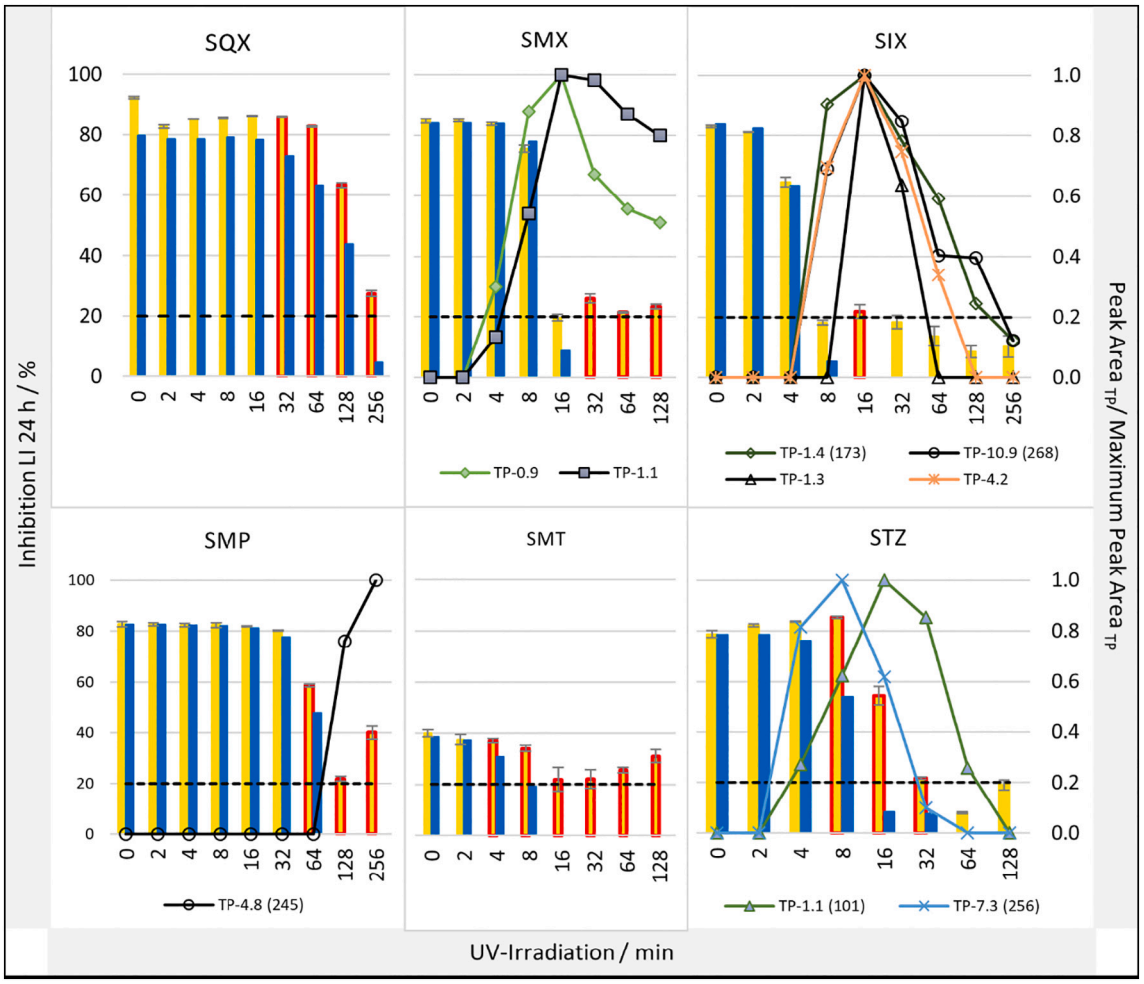

Fig. 5. Chronic luminescence inhibition (LI_{24h}) by UV-mixtures of SUAs (yellow bars), and concentration-time courses of possibly bioactive TPs. For several UV-mixtures, measured LI_{24h} can be attributed (partly) to the TP portion (red bordered yellow bares) because measured LI_{24h} was significant and ≥ 6% higher than the theoretical LI_{24h} by the PC residue (blue bars). Threshold for significant inhibition is 20% (dashed line). Raw data can be found in SI (Section 3.2).

mg L^{-1} in the LBT study by Majewsky et al. (2014). Since GI_{14h} was also low or not significant for tested UV-mixtures (with $c_{TP,i} << c_{PC,0min}$ by default; see Section 2.4), no TP was identified being significantly more active than the PC, i.e., bacteriostatic at significantly lower concentrations than PC's concentration. Note, the occurrence of TPs that are similarly bacteriostatic as the PC cannot be excluded with this study design. To refine the evaluation of the bacteriostatic effect of SUA-TPs a more sensitive test could be used in future, for example the cell proliferation inhibition test using *Escherichia coli* (MIC range: 2–512 mg L^{-1}, EUCAST database). Broth dilution methods using different pathogenic bacteria may also be suitable (e.g., Wiegand et al., 2008). Summarizing, ecotoxic effects by TPs in UV-mixtures but no bacteriostatic effects on *V. fischeri* were found.

3.3. Biodegradation test

Mineralization rates of tested SUAs and UV-mixtures, except SMX-0, were below the threshold of 60% ThOD, classifying them as not readily biodegradable (data in SI, Fig. S17a,b and Table S3). SMX-0 is considered not readily biodegradable as well although the mineralization rate was >60% ThOD but only slightly and carbon removal was significantly below the threshold of <70%. Note, when testing mixtures, the mineralization rates of a single compound remains unclear. However, rates of removal under biotic and abiotic conditions could be determined for the single compounds in the test samples based on HPLC analysis.

Starting with untreated PCs, SIX was slightly removed under biotic conditions, whereas SMP and SMX were completely removed under biotic conditions. SQX, STZ, and SMT were completely biotically removed in one test sample of the parallel determination. In the other sample, no removal of STZ and SMT, and only partial removal of SQX took place. These differences in samples A and B are also indicated by fluctuating mineralization rates.

Regarding UV-mixtures, 15 SUA-TPs were removed by >25% (i.e., PA_{d28}/PA_{d0}: 0–75%), 5 of them also under sterile conditions. The peak

Table 3
Common SUA-TPs and the parent detected in A and B samples of the parallel determination with decreased PA (green), increased PA (blue) or similar PA (grey) after 28 days, MRT. For SIX, 3 isomers were detected (1–3) showing different behaviour during incubation. nd: not detected.

Compound	SQX	SIX	SMP	SMX	STZ	SMT
NH_2-R	A B	nd	A B	A B	A B	A B
OH-SUA	A B	A B	A B	A B	A B	A B
SUA-Isomer	nd	1 2 3	nd	A B	A B	nd
Parent	A B	A B	A B	A B	A B	A B

Table 4
Mapping of data on structure, MRT and LBT of SUA-TPs. Highlighted in blue: TPs with the possibility of becoming a BbD candidate due to structure properties not contradicting BbD (yellow) and decreased peak area (↓PA, green) or possible contribution to luminescence inhibition (LI) (red). Within the group of TPs lacking structural information (see "na") there was no TP with ↓PAs (light green) and contribution to LI, thus, no TP of interest for BbD (see Section 2.7).

Sample	Name	Structure		MRT[i] PA_{d28}/PA_{d0}/%				LBT
		Structure proposal (not applicable (na))	Structure properties not of BbD interest: no SUA moiety (1), SUA-isomers (2); not applicable (na)	MRT Test Sample A	B	sterile	Conclusion a: abiotic, b: biotic	LI_{30min} LI_{24h}
-0	SQX (11.6, 301)			67	0	100	↓PA (b)	
				5	5	75	↓PA (b)	
SQX-256	TP-1.8 (161)	OH-2-amino-quinoxaline	1	110	167	78	↑PA (b)	
	TP-2.9 (146)	2-amino-quinoxaline	1	222	260	109	↑PA (b)	
	TP-7.3 (317)	OH-SQX	BbD	148	182	129	↑PA (b,a)	
	TP-7.8 (237)	desulfo-SQX	1	4	4	0	↓PA (b,a)	
	TP-10.3 (238)	Δm/z: -63, desulfo-4-OH-SQX	1	754	826	455	↑PA (b,a)	
	TP-10.7 (315)	NO-SQX	BbD	108	110	91	-PA (b,a)	
	TP-3.2	na	na	98	98	87	-PA (b,a)	
-0	SIX (10.7, 268)			101	100	100	-PA (b,a)	
				not present in SIX-16				
SIX-16	TP-1.2 (286)	Δm/z: +18 (1)	BbD	65	62	191	↓PA (b)	
	TP-1.4 (173)	SAA	BbD	144	101	136	inconclusive	LI_{24h}
	TP-3.2 (286)	Δm/z: +18 (2)	BbD	124	118	103	-PA (b,a)	
	TP-6.2 (268)	SIX-isomer (1)	2	124	120	90	-PA (b,a)	
	TP-7.0 (140)	nitrophenol	1	385	371	nd	↑PA (b)	
	TP-7.0 (268)	SIX-isomer (2)	2	422	400	nd	↑PA (b)	
	TP-10.3 (284)	OH-SIX	BbD	0	0	0	↓PA (b,a)	
	TP-10.9 (268)	SIX-isomer (3)	2	1	1	6	↓PA (b,a)	LI_{24h}
	TP-0.9	na	na	56	52	101	↓PA (b)	
	TP-1.8	na	na	44	65	74	↓PA (b,a)	
	TP-3.2	na	na	107	129	123	-PA (b,a)	
-0	SMP (8.8, 281)			0	0	94	↓PA (b)	
				0	0	99	↓PA (b)	
SMP-64	TP-1.3 (126)	3-amino-6-me-thoxypyridazine	1	394	398	105	↑PA (b)	
	TP-2.4 (233)	OH-desulfo-SMP	1	38	40	114	↓PA (b)	
	TP-3.2 (217)	desulfo-SMP	1	102	102	102	-PA (b,a)	
	TP-3.9 (297)	OH-SMP (1)	BbD	96	98	121	-PA (b,a)	
	TP-4.8 (245)	Δm/z: -36	1	48	52	28	↓PA (b,a)	LI_{30min}, LI_{24h}
	TP-9.1 (295)	NO-SMP	BbD	99	104	87	-PA (b,a)	
	TP-0.9	na	na	86	111	100	-PA (b,a)	LI_{24h}
	TP-1.1	na	na	181	209	nd	↑PA (b)	LI_{24h}
-0	SMX (10.1, 254)			0	0	100	↓PA (b)	
				0	0	108	↓PA (b)	
SMX-8	TP-1.0 (99)	3-amino-5-methyl-isoxazole	1	116	111	91	-PA (b,a)	
	TP-1.3 (286)	OH-OH-SMX	BbD	211	217	287	↑PA (b,a)	
	TP-1.9 (99)	2-amino-5-	1	311	307	110	↑PA (b)	

		methyloxazole						
	TP-4.1 (254)	SMX-isomer	2	0	0	134	↓PA (b)	
	TP-9.5 (270)	OH-SMX	BbD	0	0	136	↓PA (b)	
	TP-0.9	na	na	58	101	116	inconclusive	LI24h
	TP-1.1	na	na	82	94	124	-PA (b,a)	LI24h
	TP-2.1	na	na	70	87	116	-PA (b,a)	
-0	STZ (4.5, 256)			0	104	99	inconclusive	
				0	0	116	↓PA (b)	
STZ-16	TP-1.1 (101)	2-aminothiazole	1	257	262	125	↑PA (b)	LI_{24h}
	TP-3.6 (272)	OH-STZ	BbD	36	0	160	↓PA (b), ↑PA (a)	LI_{30min}
	TP-7.3 (256)	STZ-isomer	2	39	21	110	↓PA (b)	LI_{30min}, LI_{24h}
	TP-1.1	na	na	50	60	nd	↓PA (b)	
-0	SMT (8.5, 271)			99	0	101	inconclusive	
				110	110	104	-PA (b,a)	
SMT-16	TP-1.2 (116)	2-amino-5-methyl-1,3,4-thiadiazole	1	106	104	103	-PA (b,a)	
	TP-2.0 (207)	desulfo-SMT	1	83	72	211	-PA (b), ↑PA (a)	
	TP-3.5 (312)	Δm/z: +41	BbD	91	93	83	-PA (b,a)	
	TP-4.3 (158)	4-amino-benzene-sulfinate	1	41	60	112	↓PA (b)	
	TP-7.7 (287)	OH-SMT	BbD	130	123	137	↑PA (b,a)	
	TP-0.9	na	na	42	41	114	↓PA (b)	

[i]MRT conclusion on decreased (↓), increased (↑), or constant (−) peak area (PA) after 28 days incubation is based on PA_{d28}/PA_{d0} quotient of test sample A, B and sterile control with 0–75% ↓PA, 76–125% -PA, or > 125% ↑PA.

areas (PAs) of 12 SUA-TPs increased by at least >25% (i.e., $PA_{d28}/PA_{d0} \geq 126\%$), for 4 of them also under sterile conditions. The PAs of 15 SUA-TPs kept constant (i.e., PA_{d28}/PA_{d0}: 76–125%) (Table 4, column "MRT").

Comparing HPLC results of UV-mixtures from different SUAs let to patterns for similar TPs (Table 3). Amines NH_2-R (R: specific functional group), detected for 5 SUAs, generally increased in PA during incubation, while hydroxylated SUAs (OH-SUA, OH position not clear) and SUA-isomers, detected for 3 SUAs, rather decreased. The latter are likely structural similar to the PCs which showed also the tendency to decrease in PA.

Mineralization rates of SAA and hydroxylated SAA derivates – tested to investigate the effect of hydroxylation on SAA's biodegradability – were ≤ 20%, all classifying as not readily biodegradable. Removal under biotic conditions only (considered primary biodegradation) was observed but was still incomplete. With about 50% primary degradation, 4A3OH-BS and 2AP4-S were better primarily biodegradable than 4OH-BS and SAA with about 10% and < 5%, respectively.

3.3.1. *Insights from MRT*

Mineralization of SUAs and their UV-mixtures as well as removal rates of detected compounds were investigated successfully by MRT and subsequent HPLC-UV-MS^n analysis. The finding that tested SUAs (SUA-0) were not readily biodegradable is in line with literature (Ingerslev and Halling-Sørensen, 2000). The sulfanilamide core structure as well as sulfanilic acid can be expected to degrade very slowly in water (National Center for Biotechnology Information, 2023b, 2023c). This demonstrates SUA's resistance to complete biodegradation (National Center for Biotechnology Information, 2023a, 2023b, 2023c).

SUAs showed the tendency of complete primary elimination under biotic conditions. Due to the observed incomplete biodegradation, the primary elimination should have led to not degraded TPs and/or adsorption on the sludge. The reason for primary elimination could be SUA-adapted bacteria due to exposure to SUAs in Lüneburg's WWTP leading to growth of specific SUA-degraders (García Galán et al., 2012; Ingerslev and Halling-Sørensen, 2000). The occurrence of specific SUA-degraders could also explain the disappearance of structurally similar TPs (OH-SMX, OH-STZ, SMX-, and STZ-isomer) under biotic conditions (Table 4) as it was found that enzymes involved in SUA's degradation are class-specific rather than compound-specific (Ingerslev and Halling-Sørensen, 2000).

Amines NH_2-R (R: specific functional group) of 4 SUAs were formed likely due to δ-cleavage of SUAs or SUA-related TPs, which is in line with literature describing the amines NH_2-R as dead-end TP of SUA's biodegradation (Ricken et al., 2013). Only for SIX, the corresponding NH_2-R (5-amino-3,4-dimethylisoxazole) was not detected in the UV-mixture used for the MRT (SIX-16). This can be explained by SIX-16 being free of PC in contrast to the UV-mixtures of the other PCs.

4. TPs of interest for BbD and future research

Based on LBT and MRT results and considering structural features not contradicting BbD (see method 2.7), five TPs were of interest for BbD due to removal in the MRT and/or possible contribution to luminescence inhibition, requiring a closer look (Table 4, blue highlighted). Among them were SIX-TP-10.3, SMX-TP-9.5, and STZ-TP-3.6, proposed to be hydroxylated (OH-SIX, -SMX, -STZ), due to differences in *m/z* to the PC of +16. Bioactivity wasn't concluded based on the comparison of LBT data and their c-t curves (see Section 3.2) but cannot be excluded because their concentrations in the UV-mixtures may have been too low to inhibit bacterial luminescence (cf. SI, Figs. S3, S5, S6). In addition, single hydroxylation of a SUA is only a slight structural change, and might not reduce the bacteriostatic efficacy of the PC significantly. For example, Majewsky et al. (2014) found *N4*-OH-SMX to be similarly bioactive as SMX. Hydroxylated TPs were assumed, to some extent, to decrease during incubation because of the rule of thumb that

oxygenation favours biodegradability. There is no generic rule for the number and position of a substituent, e.g., regarding hydroxy group(s) at a phenyl ring, but they are known to influence biodegradability depending on the base structure (Boethling et al., 2007). The subtle rule of thumb on oxygenation didn't apply to tested hydroxylated SAA-derivatives (Fig. 2), whose hydroxylation in terms of degree and position didn't result in increased mineralization rate. Therefore, disappearance of OH-SUAs (OH-SIX, -SMX, -STZ) during MRT (Table 4) was likely only due to further transformation and/or adsorption on sludge but not mineralization, excluding them as BbD candidate.

The remaining TPs of interest for BbD were SIX-TP-1.2 (286) and SIX-TP-1.4 (173) (Table 4, blue highlighted). The latter is proposed to be SAA. According to literature data (National Center for Biotechnology Information, 2023b), SAA is predicted not to biodegrade readily in the aquatic environment. This excludes TP-1.4 (173) as BbD candidate. A closer look at the mass spectrum of TP-1.2 (286) revealed that the fragments characteristic for the SAA core structure (m/z = 156, 113, 108) were still present. This indicates an unchanged SAA structure, but slightly modified specific functional group ($\Delta m/z = +18$; additional fragments with m/z = 241, 243), which is an excluding criterion for structures of interest for BbD (see Section 2.7). Thus, no BbD candidate was identified using this effect-driven approach.

When redesigning SUAs by generating derivatives through photo-transformation, improving environmental biodegradability was considered more challenging than retaining bioactivity. The MRT evaluation of UV-mixtures didn't result in the identification of a candidate for better biodegradability, whereas the LBT indicated bioactive TPs and also other studies identified bacteriostatic SUA-TPs (see LBT insights). Identifying improving biodegradability as the limiting factor of the BbD approach may help steer future research on the redesign of SUAs and BbD of antibiotics in general in the following way:

Primarily, future work should aim for better biodegradability by targeted modification of the sulfonamide structure. More specifically, modified SUA would first have to be deactivated by an abiotic transformation step (e.g., photolysis or hydrolysis; compare Leder et al., 2021). Generated inactive TPs should then mineralize readily by subsequent enzymatic processes in order to avoid chemical pollution of the environment. The reason for this stepwise approach is to avoid biodegradation acting as a mechanism of antibiotic resistance (Ricken et al., 2017; Vila-Costa et al., 2017).

Secondly, bacteriostatic efficacy could be tested on molecules that are degradable. Even a modification of the pharmacophore might be possible (cf. findings by Majewsky et al., 2014) as long as features relevant for pharmacological properties, e.g., the target binding (SUA-dihydropteroate synthase complex), remain.

An important lesson learnt from this study for BbD in general is that, although bioactive TP-mixtures and removal rates of single TPs can be determined via LBT and MRT, respectively, it is challenging to find any hints to specific benign TPs based on data from complex mixtures. This is where future work could start. For example, as a variation of the non-targeted design approach, UV-mixtures of interest could be fractionated chromatographically or using solid phase extraction so that selected fractions with significantly reduced TP diversity are screened for bioactivity and (bio)degradability. The targeted design approach (cf. Lorenz et al., 2021) could also be applied by modifying the PC based on expertise and then prioritizing a promising structure for synthesis through computational methods. In the targeted approach, the pharmacophore could also undergo a change (see paragraph above). For this purpose, collaboration between environmental scientists and drug design experts would be helpful.

5. Conclusion

The objective of this study was to broaden the understanding of the redesign approach within BbD using sulfonamide antibiotics (SUAs) as an example. Applied methodology was beneficial in terms of simultaneous generation and subsequent screening of many transformation products of six SUAs which are hardly commercially available. Searching for indications on possibly better biodegradable TPs, limited significance of mixture tests for a single compound was accepted. Based on biodegradability testing (manometric respirometry test, MRT) and screening of antibiotic activity needed for application (luminescence bacteria test, LBT), no photo-TP was indicated as a potentially greener alternative for SUAs.

Gained insights from MRT and LBT support the understanding of SUAs and SUA-TPs and future work on SUA's redesign. It was also found that photo-TPs can be ecotoxic while being not removable under biotic conditions. Even hydroxylated derivatives of SAA, assumed to be better biodegradable and therefore tested as a single compound, were not readily biodegradable. This demonstrates that known rules of thumb can give general guidance and have to be checked on a case-by-case basis. The specific results underline the high stability of the sulfonamide moiety against environmental biodegradation.

CRediT authorship contribution statement

Neele Puhlmann: Writing – original draft, Methodology, Investigation, Conceptualization. **Oliver Olsson:** Writing – review & editing, Supervision, Methodology, Conceptualization. **Klaus Kümmerer:** Writing – review & editing, Supervision, Methodology, Conceptualization, Funding acquisition.

Declaration of competing interest

The authors declare that they have no known competing financial interests or personal relationships that could have appeared to influence the work reported in this paper.

Data availability

Data will be made available on request.

Appendix A. Supplementary data

Supplementary data to this article can be found online at https://doi.org/10.1016/j.scitotenv.2024.171027.

References

Achermann, S., Bianco, V., Mansfeldt, C.B., Vogler, B., Kolvenbach, B.A., Corvini, P.F.X., Fenner, K., 2018. Biotransformation of sulfonamide antibiotics in activated sludge: the formation of Pterin-conjugates leads to sustained risk. Environ. Sci. Technol. 52 (11), 6265–6274.

Anastas, P.T., Warner, J.C. (Eds.), 1998. Green Chemistry: Theory and Practice. Oxford University Press, Oxford [England], New York.

Baena-Nogueras, R.M., González-Mazo, E., Lara-Martín, P.A., 2017. Photolysis of antibiotics under simulated sunlight irradiation: identification of photoproducts by high-resolution mass spectrometry. Environ. Sci. Technol. 51 (6), 3148–3156.

Balouiri, M., Sadiki, M., Ibnsouda, S.K., 2016. Methods for in vitro evaluating antimicrobial activity: A review. Journal of Pharmaceutical Analysis 6 (2), 71–79.

Baran, W., Adamek, E., Ziemiańska, J., Sobczak, A., 2011. Effects of the presence of sulfonamides in the environment and their influence on human health. J. Hazard. Mater. 196, 1–15.

Boethling, R.S., Sommer, E., DiFiore, D., 2007. Designing small molecules for biodegradability. Chem. Rev. 107 (6), 2207–2227.

Bonvin, F., Omlin, J., Rutler, R., Schweizer, W.B., Alaimo, P.J., Strathmann, T.J., McNeill, K., Kohn, T., 2013. Direct photolysis of human metabolites of the antibiotic sulfamethoxazole: evidence for abiotic back-transformation. Environ. Sci. Technol. 47 (13), 6746–6755.

Boreen, A.L., Arnold, W.A., McNeill, K., 2004. Photochemical fate of sulfa drugs in the aquatic environment: sulfa drugs containing five-membered heterocyclic groups. Environ. Sci. Technol. 38 (14), 3933–3940.

Boreen, A.L., Arnold, W.A., McNeill, K., 2005. Triplet-sensitized photodegradation of sulfa drugs containing six-membered heterocyclic groups: identification of an SO2 extrusion photoproduct. Environ. Sci. Technol. 39 (10), 3630–3638.

Calza, P., Medana, C., Pazzi, M., Baiocchi, C., Pelizzetti, E., 2004. Photocatalytic transformations of sulphonamides on titanium dioxide. Appl. Catal. Environ. 53 (1), 63–69.

Christou, A., Michael, C., Fatta-Kassinos, D., Fotopoulos, V., 2018. Can the pharmaceutically active compounds released in agroecosystems be considered as emerging plant stressors? Environ. Int. 114, 360–364.
Cycoń, M., Mrozik, A., Piotrowska-Seget, Z., 2019. Antibiotics in the soil environment-degradation and their impact on microbial activity and diversity. Front. Microbiol. 10, 338.
Deng, F., Qiu, S., Olvera-vargas, H., Zhu, Y., Gao, W., Yang, J., Ma, F., 2019. Electrocatalytic sulfathiazole degradation by a novel nickel-foam cathode coated with nitrogen-doped porous carbon. Electrochim. Acta 297, 21–30.
European Commission, 2020a. Communication from the Commission to the European Parliament, the Council, the European Economic and Social Committee and the Committee of the Regions: Chemicals Strategy for Sustainability Towards a Toxic-Free Environment (accessed 18.02.2021). https://ec.europa.eu/environment/pdf/chemicals/2020/10/Strategy.pdf.
European Commission, 2020b. Pharmaceutical Strategy for Europe (accessed 4.05.2023). https://ec.europa.eu/commission/presscorner/detail/en/ip_20_2173.
Ezzariai, A., Hafidi, M., Khadra, A., Aemig, Q., El Fels, L., Barret, M., Merlina, G., Patureau, D., Pinelli, E., 2018. Human and veterinary antibiotics during composting of sludge or manure: global perspectives on persistence, degradation, and resistance genes. J. Hazard. Mater. 359, 465–481.
Fabbri, D., López-Muñoz, M.J., Daniele, A., Medana, C., Calza, P., 2019. Photocatalytic abatement of emerging pollutants in pure water and wastewater effluent by TiO2 and Ce-ZnO: degradation kinetics and assessment of transformation products. Photochem. Photobiol. Sci. 18 (4), 845–852.
Felis, E., Kalka, J., Sochacki, A., Kowalska, K., Bajkacz, S., Harnisz, M., Korzeniewska, E., 2020. Antimicrobial pharmaceuticals in the aquatic environment - occurrence and environmental implications. Eur. J. Pharmacol. 866, 172813.
Finckh, S., Beckers, L.-M., Busch, W., Carmona, E., Dulio, V., Kramer, L., Krauss, M., Posthuma, L., Schulze, T., Slootweg, J., von der Ohe, P.C., Brack, W., 2022. A risk based assessment approach for chemical mixtures from wastewater treatment plant effluents. Environ. Int. 164, 107234. https://doi.org/10.1016/j.envint.2022.107234.
Gao, Y., Gao, N., Chu, W., Zhang, Y., Zhang, J., Yin, D., 2019. UV-activated persulfate oxidation of sulfamethoxypyridazine: kinetics, degradation pathways and impact on DBP formation during subsequent chlorination. Chem. Eng. J. 370, 706–715.
García Galán, M.J., Díaz-Cruz, M.S., Barceló, D., 2012. Removal of sulfonamide antibiotics upon conventional activated sludge and advanced membrane bioreactor treatment. Anal. Bioanal. Chem. 404 (5), 1505–1515.
García-Galán, M.J., Petrovic, M., Rodríguez-Mozaz, S., Barceló, D., 2016. Multiresidue trace analysis of pharmaceuticals, their human metabolites and transformation products by fully automated on-line solid-phase extraction-liquid chromatography-tandem mass spectrometry. Talanta 158, 330–341.
Ge, L., Zhang, P., Halsall, C., Li, Y., Chen, C.-E., Li, J., Sun, H., Yao, Z., 2019. The importance of reactive oxygen species on the aqueous phototransformation of sulfonamide antibiotics: kinetics, pathways, and comparisons with direct photolysis. Water Res. 149, 243–250.
Gómez-Ramos, M.d.M., Mezcua, M., Agüera, A., Fernández-Alba, A.R., Gonzalo, S., Rodríguez, A., Rosal, R., 2011. Chemical and toxicological evolution of the antibiotic sulfamethoxazole under ozone treatment in water solution. J. Hazard. Mater. 192 (1), 18–25.
Hensen, B., Olsson, O., Kümmerer, K., 2020. A strategy for an initial assessment of the ecotoxicological effects of transformation products of pesticides in aquatic systems following a tiered approach. Environ. Int. 137, 105533.
Hu, Z., Xie, X., Li, S., Song, M., Liang, G., Zhao, J., Wang, Z., 2021. Rational construct CQDs/BiOCOOH/uCN photocatalyst with excellent photocatalytic performance for degradation of sulfathiazole. Chem. Eng. J. 404, 126541.
Ingerslev, F., Halling-Sørensen, B., 2000. Biodegradability properties of sulfonamides in activated sludge. Environ. Toxicol. Chem. 19 (10), 2467–2473.
Ji, Y., Wang, L., Jiang, M., Yang, Y., Yang, P., Lu, J., Ferronato, C., Chovelon, J.-M., 2017. Ferrous-activated peroxymonosulfate oxidation of antimicrobial agent sulfaquinoxaline and structurally related compounds in aqueous solution: kinetics, products, and transformation pathways. Environ. Sci. Pollut. Res. Int. 24 (24), 19535–19545.
Khaleel, N.D., Mahmoud, W.M., Hadad, G.M., Abdel-Salam, R.A., Kümmerer, K., 2013. Photolysis of sulfamethoxypyridazine in various aqueous media: aerobic biodegradation and identification of photoproducts by LC-UV–MS/MS. J. Hazard. Mater. 244-245, 654–661.
Klauson, D., Krichevskaya, M., Borissova, M., Preis, S., 2010. Aqueous photocatalytic oxidation of sulfamethizole. Environ. Technol. 31 (14), 1547–1555.
Kümmerer, K., 2007. Sustainable from the very beginning: rational design of molecules by life cycle engineering as an important approach for green pharmacy and green chemistry. Green Chem. 9 (8), 899–907.
Kümmerer, K., 2010. Why green and sustainable pharmacy? In: Kümmerer, K., Hempel, M. (Eds.), Green and Sustainable Pharmacy. Springer, Berlin Heidelberg, Berlin, Heidelberg, pp. 3–10.
Leder, C., Suk, M., Lorenz, S., Rastogi, T., Peifer, C., Kietzmann, M., Jonas, D., Buck, M., Pahl, A., Kümmerer, K., 2021. Reducing environmental pollution by antibiotics through Design for Environmental Degradation. ACS Sustain. Chem. Eng. 9 (28), 9358–9368.
Liao, Q.-N., Ji, F., Li, J.-C., Zhan, X., Hu, Z.-H., 2016. Decomposition and mineralization of sulfaquinoxaline sodium during UV/H2O2 oxidation processes. Chem. Eng. J. 284, 494–502.
Liu, G., Wang, H., Chen, D., Dai, C., Zhang, Z., Feng, Y., 2020. Photodegradation performances and transformation mechanism of sulfamethoxazole with CeO2/CN heterojunction as photocatalyst. Sep. Purif. Technol. 237, 116329.
Lorenz, S., Amsel, A.-K., Puhlmann, N., Reich, M., Olsson, O., Kümmerer, K., 2021. Toward application and implementation of in silico tools and workflows within benign by design approaches. ACS Sustain. Chem. Eng. 9 (37), 12461–12475.
Majewsky, M., Wagner, D., Delay, M., Bräse, S., Yargeau, V., Horn, H., 2014. Antibacterial activity of sulfamethoxazole transformation products (TPs): general relevance for sulfonamide TPs modified at the Para position. Chem. Res. Toxicol. 27 (10), 1821–1828.
Menz, J., Schneider, M., Kümmerer, K., 2013. Toxicity testing with luminescent bacteria – characterization of an automated method for the combined assessment of acute and chronic effects. Chemosphere 93 (6), 990–996.
Mirzaei, A., Chen, Z., Haghighat, F., Yerushalmi, L., 2018. Hierarchical magnetic petal-like Fe3O4-ZnO@g-C3N4 for removal of sulfamethoxazole, suppression of photocorrosion, by-products identification and toxicity assessment. Chemosphere 205, 463–474.
Nassar, R., Trivella, A., Mokh, S., Al-Iskandarani, M., Budzinski, H., Mazellier, P., 2017. Photodegradation of sulfamethazine, sulfamethoxypiridazine, amitriptyline, and clomipramine drugs in aqueous media. J. Photochem. Photobiol. A Chem. 336, 176–182.
Nassar, R., Mokh, S., Rifai, A., Chamas, F., Hoteit, M., Al Iskandarani, M., 2018. Transformation of sulfaquinoxaline by chlorine and UV light in water: kinetics and by-product identification. Environ. Sci. Pollut. Res. Int. 25 (35), 34863–34872.
National Center for Biotechnology Information, 2023a. PubChem Compound Summary for CID 5329, Sulfamethoxazole - 12.2.3 Environmental Fate (accessed 21.06.2023). https://pubchem.ncbi.nlm.nih.gov/compound/Sulfamethoxazole.
National Center for Biotechnology Information, 2023b. PubChem Compound Summary for CID 5333, Sulfanilamide - 13.2.1 Environmental Fate/Exposure Summary (accessed 20.06.2023). https://pubchem.ncbi.nlm.nih.gov/compound/Sulfanilamide.
National Center for Biotechnology Information, 2023c. PubChem Compound Summary for CID 8479, Sulfanilic Acid - 13.2.2 Environmental Fate/Exposure Summary (accessed 20.06.2023). https://pubchem.ncbi.nlm.nih.gov/compound/Sulfanilic-acid.
Niu, X.-Z., Glady-Croué, J., Croué, J.-P., 2017. Photodegradation of sulfathiazole under simulated sunlight: kinetics, photo-induced structural rearrangement, and antimicrobial activities of photoproducts. Water Res. 124, 576–583.
OECD, 2006. OECD Guidelines for the Tesing of Chemicals: Section 3, Introduction (web archive link, 18 February 2021) (accessed 18.02.2021). https://www.oecd-ilibrary.org/docserver/9789264030213-en.pdf?expires=1613640811&id=id&accname=guest&checksum=AC41CE07043A281F7A69297AFF853D6A.
Palm, W.-U., Schmidt, N., Stahn, M., Grimme, S., 2023. A kinetic study of the photolysis of sulfamethoxazole with special emphasis on the photoisomer. Photochem. Photobiol. Sci. 22 (3), 615–630.
Puhlmann, N., Mols, R., Olsson, O., Slootweg, J.C., Kümmerer, K., 2021. Towards the design of active pharmaceutical ingredients mineralizing readily in the environment. Green Chem. 23 (14), 5006–5023. https://doi.org/10.1039/D1GC01048D.
Puhlmann, N., Olsson, O., Kümmerer, K., 2022. Transformation products of sulfonamides in aquatic systems: lessons learned from available environmental fate and behaviour data. Sci. Total Environ. 830, 154744.
Qiu, W., Zheng, M., Sun, J., Tian, Y., Fang, M., Zheng, Y., Zhang, T., Zheng, C., 2019. Photolysis of enrofloxacin, pefloxacin and sulfaquinoxaline in aqueous solution by UV/H(2)O(2), UV/Fe(II), and UV/H(2)O(2)/Fe(II) and the toxicity of the final reaction solutions on zebrafish embryos. Sci. Total Environ. 651 (Pt 1), 1457–1468.
Radke, M., Lauwigi, C., Heinkele, G., Mürdter, T.E., Letzel, M., 2009. Fate of the antibiotic sulfamethoxazole and its two major human metabolites in a water sediment test. Environ. Sci. Technol. 43 (9), 3135–3141.
Rastogi, T., Leder, C., Kümmerer, K., 2014. Designing green derivatives of β-blocker metoprolol: a tiered approach for green and sustainable pharmacy and chemistry. Chemosphere 111, 493–499.
Ricken, B., Corvini, P.F.X., Cichocka, D., Parisi, M., Lenz, M., Wyss, D., Martínez-Lavanchy, P.M., Müller, J.A., Shahgaldian, P., Tulli, L.G., Kohler, H.-P.E., Kolvenbach, B.A., 2013. Ipso-hydroxylation and subsequent fragmentation: a novel microbial strategy to eliminate sulfonamide antibiotics. Appl. Environ. Microbiol. 5550–5558.
Ricken, B., Kolvenbach, B.A., Bergesch, C., Benndorf, D., Kroll, K., Strnad, H., Vlček, Č., Adaixo, R., Hammes, F., Shahgaldian, P., Schäffer, A., Kohler, H.-P.E., Corvini, P.F.-X., 2017. FMNH(2)-dependent monooxygenases initiate catabolism of sulfonamides in Microbacterium sp. strain BR1 subsisting on sulfonamide antibiotics. Sci. Rep. 7 (1), 15783.
Spielmeyer, A., 2018. Occurrence and fate of antibiotics in manure during manure treatments: A short review. Sustain. Chem. Pharm. 9, 76–86.
Spielmeyer, A., Heer, M., Mohring, S.A., Hausmann, H., Stahl, J., Kietzmann, M., Dold, S., Spengler, B., Hamscher, G., 2015. UV-irradiation of the antibiotic sulfathiazole surprisingly leads to former Antituberculotic Promizole. Clean Soil Air Water 43 (4), 490–495.
Su, T., Deng, H., Benskin, J.P., Radke, M., 2016. Biodegradation of sulfamethoxazole photo-transformation products in a water/sediment test. Chemosphere 148, 518–525.
Urbano, V.R., Maniero, M.G., Pérez-Moya, M., Guimarães, J.R., 2017a. Influence of pH and ozone dose on sulfaquinoxaline ozonation. J. Environ. Manage. 195 (Pt 2), 224–231.
Urbano, V.R., Peres, M.S., Maniero, M.G., Guimarães, J.R., 2017b. Abatement and toxicity reduction of antimicrobials by UV/H(2)O(2) process. J. Environ. Manage. 193, 439–447.
Vila-Costa, M., Gioia, R., Aceña, J., Pérez, S., Casamayor, E.O., Dachs, J., 2017. Degradation of sulfonamides as a microbial resistance mechanism. Water Res. 115, 309–317.

Wang, J., Gong, Q., Ali, J., Shen, M., Cai, J., Zhou, X., Liao, Z., Wang, S., Chen, Z., 2020. pH-dependent transformation products and residual toxicity evaluation of sulfamethoxazole degradation through non-radical oxygen species involved process. Chem. Eng. J. 390, 124512.

Wang, W., Tian, J., Zhu, Z., Zhu, C., Liu, B., Hu, C., 2021. Insight into quinolones and sulfonamides degradation, intermediate product identification and decomposition pathways with the assistance of Bi2MoO6/Bi2WO6/MWCNTs photocatalyst. Process Saf. Environ. Prot. 147, 527–546.

Wiegand, I., Hilpert, K., Hancock, R.E.W., 2008. Agar and broth dilution methods to determine the minimal inhibitory concentration (MIC) of antimicrobial substances. Nat. Protoc. 3 (2), 163–175.

Wilkinson, J.L., Boxall, A.B.A., Kolpin, D.W., Leung, K.M.Y., La, i.R.W.S., Galbán-Malagón, C., Adell, A.D., Mondon, J., Metian, M., Marchant, R.A., Bouzas-Monroy, A., Cuni-Sanchez, A., Coors, A., Pedro, Carriquiriborde, Rojo, M., Gordon, C., Cara, M., Moermond, M., Luarte, T., Petrosyan, V., Perikhanyan, Y., Mahon, C.S., McGurk, C.J., Hofmann, T., Kormoker, T., Iniguez, V., Guzman-Otazo, J., Tavares, J.L., Gildasio De Figueiredo, F., Razzolini, M.T.P., Dougnon, V., Gbaguidi, G., Traoré, O., Blais, J.M., Kimpe, L.E., Wong, M., Wong, D., Ntchantcho, R., Pizarro, J., Ying, G.-G., Chen, C.-E., Páez, M., Martínez-Lara, J., Otamonga, J.-P., Poté, J., Ifo, S.A., Wilson, P., Echeverría-Sáenz, S., Udikovic-Kolic, N., Milakovic, M., Fatta-Kassinos, D., Ioannou-Ttofa, L., Belušová, V., Vymazal, J., Cárdenas-Bustamante, M., Kassa, B.A., Garric, J., Chaumot, A., Gibba, P., Kunchulia, I., Seidensticker, S., Lyberatos, G., Halldórsson, H.P., Melling, M., Shashidhar, T., Lamba, M., Nastiti, A., Supriatin, A., Pourang, N., Abedini, A., Abdullah, O., Gharbia, S.S., Pilla, F., Chefetz, B., Topaz, T., Yao, Koffi, Marcellin, Aubakirova, B., Beisenova, R., Olaka, L., Mulu, J.K., Chatanga, P., Ntuli, V., Blama, N.T., Sherif, S., Aris, A.Z., Looi, L.J., Niang, M., Traore, S.T., Oldenkamp, R., Ogunbanwo, O., Ashfaq, M., Iqbal, M., Abdeen, Z., O'Dea, A., Morales-Saldaña, J.M., Custodio, M., La Cruz, H. de, Ian, Navarrete, Carvalho, F., Gogra, A.B., Koroma, B.M., Cerkvenik-Flajs, V., Gombač, M., Thwala, M., Choi, K., Kang, H., Ladu, J.L.C., Rico, A., Amerasinghe, P., Sobek, A., Horlitz, G., Zenker, A.K., King, A.C., Jiang, J.-J., Kariuki, R., Tumbo, M., Tezel, U., Onay, T.T., Lejju, J.B., Vystavna, Y., Vergeles, Y., Heinzen, H., Pérez-Parada, A., Sims, D.B., Figy, M., Good, D., Teta, C., 2022. Pharmaceutical pollution of the world's rivers. Proc. Natl. Acad. Sci. 119 (8), e2113947119.

Yang, H., Li, G., An, T., Gao, Y., Fu, J., 2010. Photocatalytic degradation kinetics and mechanism of environmental pharmaceuticals in aqueous suspension of TiO2: A case of sulfa drugs. Catal. Today 153 (3), 200–207.

Yao, J., Zeng, X., Wang, Z., 2017. Enhanced degradation performance of sulfisoxazole using peroxymonosulfate activated by copper-cobalt oxides in aqueous solution: kinetic study and products identification. Chem. Eng. J. 330, 345–354.

Zhang, R., Yang, Y., Huang, C.-H., Li, N., Liu, H., Zhao, L., Sun, P., 2016. UV/H2O2 and UV/PDS treatment of trimethoprim and sulfamethoxazole in synthetic human urine: transformation products and toxicity. Environ. Sci. Technol. 50 (5), 2573–2583.

Zhou, W., Moore, D.E., 1994. Photochemical decomposition of sulfamethoxazole. Int. J. Pharm. 110 (1), 55–63.